

# Development of Coherent 2- $\mu\text{m}$ Differential Absorption and Wind Lidar with laser frequency offset locking technique and column-integrated CO<sub>2</sub> measurement

S. Ishii<sup>1</sup>, K. Mizutani<sup>1</sup>, H. Fukuoka<sup>2</sup>, T. Ishikawa<sup>3</sup>, P. Baron<sup>1</sup>, T. Tanaka<sup>4,\*</sup>,  
I. Morino<sup>4</sup>, O. Uchino<sup>4</sup>, H. Iwai<sup>1</sup>, T. Aoki<sup>1</sup>, T. Itabe<sup>1</sup>, A. Sato<sup>5</sup>, and K. Asai<sup>5</sup>

<sup>1</sup> National Institute of Information and Communications Technology, Koganei-shi JAPAN

<sup>2</sup> Hamamatsu Photonics K.K., Hamamatsu-shi Japan

<sup>3</sup> Nippon Aleph Co., Yokohama-shi Japan

<sup>4</sup> National Institute for Environmental Studies, Tsukuba-shi Japan

<sup>5</sup> Tohoku Institute of Technology, Sendai-shi Japan

\* Present affiliation: Japan Aerospace Exploration Agency, Tsukuba-shi Japan  
Email: sishii@nict.go.jp

## 1. Introduction

Global spatial and temporal variations of the CO<sub>2</sub> concentration are important to understand the carbon cycle and to estimate the carbon flux. Spaceborne measurement is a promising approach to globally measure the temporal and spatial distribution of CO<sub>2</sub> concentration (XCO<sub>2</sub>: column-weighted dry-air mixing ratio of CO<sub>2</sub>). Global sensitivity experiments have indicated that spaceborne measurements with a bias-free high precision less than 1% can help improve the accuracy of CO<sub>2</sub> flux estimates [1-3]. In January 2009, the Greenhouse gas Observing SATellite (GOSAT) [4] equipped with spaceborne passive sensors was launched to monitor the global total column CO<sub>2</sub> concentration continuously and the Orbiting Carbon Observatory-2 [5] will be also launched for the same purpose no later than February 2013. The passive sensor is affected by aerosols and thin clouds: those presences modify the optical depth and XCO<sub>2</sub> data could be biased easily.

Differential absorption lidar (DIAL) is regarded as one of the next-generation spaceborne sensors to measure CO<sub>2</sub> concentration and has the potential advantage of providing a high measurement accuracy. 1.6- $\mu\text{m}$  and 2- $\mu\text{m}$  DIAL systems have been developing by various research groups [6-13]. The weighting function of CO<sub>2</sub> absorption cross section indicates that the spectral region of 2- $\mu\text{m}$  is suitable for lower tropospheric measurement. We developed a coherent 2- $\mu\text{m}$  differential absorption and wind lidar (Co2DiaWiL) with laser offset locking technique

to make long-range CO<sub>2</sub> measurement. In this paper, we present improvements of the Co2DiaWiL for a long-range CO<sub>2</sub> measurement and also describe examples of vertical measurements.

## 2. Coherent 2- $\mu\text{m}$ differential absorption and wind lidar

Specifications and a block diagram of the Co2DiaWiL are shown in Table 1 and Figure 1, respectively. The Co2DiaWiL has three diode-pumped single-frequency continuous-wave (CW) Tm,Ho:YLF lasers, a Q-switched Tm,Ho:YLF laser, a Mersenne off-axis telescope with a 10-cm aperture, a two-axis scanning device, two heterodyne detectors, and signal processing devices. The single-frequency Q-switched Tm,Ho:YLF laser with an operating wavelength of 2.05  $\mu\text{m}$  demonstrates an output energy of 80 mJ with a pulse width of 150 ns (FWHM) at a pulse repetition frequency of 30 Hz. The Tm,Ho:YLF laser rod in the pumping cavity, which is placed in a vacuum container, is side-pumped by 12 InGaAs/GaAs laser diode arrays. The laser rod and the diode arrays in the pumping cavity are conductively-cooled to -80 °C and approximately 20 °C, respectively. The Q-switched Tm,Ho:YLF laser uses the injection seeding for obtaining single frequency operation. The three diode-pumped single-frequency CW Tm,Ho:YLF lasers (MOs) are used for the injection seeding and referred to  $\lambda$ -center, on-line, and off-line lasers. The wavelength of the  $\lambda$ -center laser is set at 2050.967 nm to correspond to the R30 absorption line center of CO<sub>2</sub>. The frequency stabilization of the  $\lambda$ -center determines the

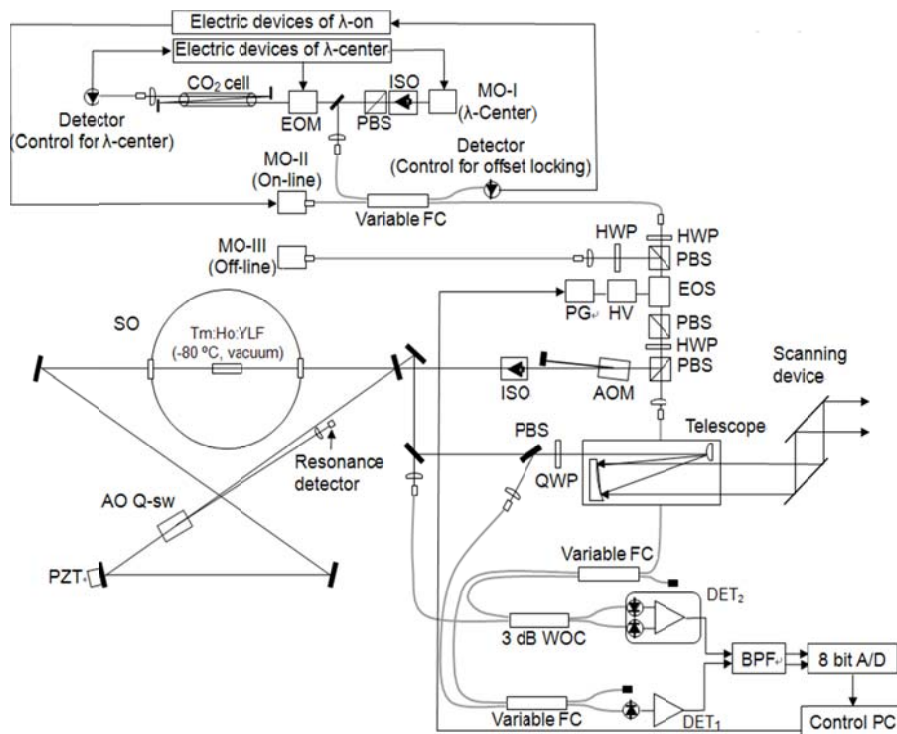


Figure 1 Block diagram of coherent 2- $\mu\text{m}$  differential absorption and wind lidar

Table 1 Specifications of coherent 2- $\mu\text{m}$  differential absorption and wind lidar

<b>Transmitter</b>	
Laser	: Tm:Ho:YLF
Wavelength	: 2051.004 to 2051.060 nm (On) : 2051.250 nm (Off)
Pulse energy	: 80 mJ/pulse
Pulse width	: 150 nsec
Pulse Repetition	: 30 Hz
<b>Receiver</b>	
Clear diameter	: 10 cm $\Phi$
Detector	: InGaAs PIN PD
<b>Data Processing</b>	
Signal processing	: 8 Bit A/D
Sampling frequency	: 500 MHz
Sampling points	: 131072
<b>Scanner</b>	
Clear diameter	: 10 cm $\Phi$
Elevation angle	: -20-200°
Azimuth angle	: -10-370°
Scanning speed	: 0°-60°/sec

frequency stabilization of the on-line laser. The  $\lambda$ -center laser is well-tuned by using a 40-cm-long containing pure  $\text{CO}_2$  at 20 torr, an external phase modulation (EOM), PID controller, PZT driver, and electric devices. The frequency stabilization of the  $\lambda$ -center laser was locked within about 160 KHz. The tunable on-line wavelength is generated by laser frequency

offsetting the on-line laser from the R30 absorption line centre. The laser frequency offset can be selected in the range of 2.5 to 6.5 GHz. The frequency stabilization of the  $\lambda$ -on laser can be locked within about 100 KHz for the  $\lambda$ -center laser. The square root of the sum of the frequency variances of the  $\lambda$ -center and  $\lambda$ -on lasers was within 190 KHz. The wavelength of the off-line laser is set at 2051.250 nm to correspond to the far wing of the R30 absorption line. The interference due to the presence of other atmospheric gases can be negligible. The on-line and off-line lasers entering an electro-optic switch (EOS,  $\text{LiNbO}_3$ ) are horizontal- and vertical- linearly-polarized lights, respectively. Those pulses were alternately switched every 1 shot. The pulsed laser beam is emitted into the atmosphere by using the telescope and a waterproof two-axis scanner. The signal backscattered by moving aerosol particles is photomixed with a portion of the on- and off-line lasers on an InGaAs PIN photodiode ( $\text{DET}_1$ ) (Hamamatsu: C5658-4973). The heterodyne detection is operated under the shot noise limited condition. A balanced InGaAs photoreceiver ( $\text{DET}_2$ ) is used for monitoring the frequency of the outgoing laser pulse. The outputs of  $\text{DET}_1$  and  $\text{DET}_2$  are digitized at 500

MHz by using 8-bit analog-to-digital (A/D) converters. The power spectra of the laser pulses (on-line and off-line pulses) and backscattered signals were obtained by 4096- and 256-point fast Fourier transforms (FFTs). The 256-point FFT corresponds to a range resolution of 75m along the line-of-sight. An algorithm proposed by Frehlich et al. [14] was used to estimate the power of the backscattered signals.

### 3. Estimation of XCO<sub>2</sub>

The differential absorption optical depth (DAOD)  $\tau$  due to the CO<sub>2</sub> absorption from R<sub>1</sub> to R<sub>2</sub> is given by

$$\tau(R_1, R_2) = \int_{R_1}^{R_2} n_{CO_2} \{ \sigma_{on}(r) - \sigma_{off}(r) \} dr = \frac{1}{2} \cdot \log \left( \frac{P_{on}(R_1) \cdot P_{off}(R_2)}{P_{off}(R_1) \cdot P_{on}(R_2)} \right),$$

where  $\sigma_i(r)$  is the absorption cross section of CO<sub>2</sub> molecules,  $n$  is the CO<sub>2</sub> number density, and  $P_i = P_{on}, P_{off}(r)$  is power of the backscattered signal received at range R. The XCO<sub>2</sub> is given by

$$XCO_2 = \frac{\int_{R_1}^{R_2} n_{CO_2}(r) \cdot WF(r) dr}{\int_{R_1}^{R_2} WF(r) dr} = \frac{\tau}{\int_{R_1}^{R_2} n_{air}(r) \cdot \Delta\sigma dr}$$

where WF is the weighting function,  $n_{air}$  is the dry-air number densities, and  $\Delta\sigma (= \sigma_{on}(r) - \sigma_{off}(r))$  is the difference between the absorption cross sections corresponding to the wavelengths of the on-line and off-line lasers.

### 4. Result

Figure 2 shows an example of the atmospheric returns corresponding to the off-line laser and on-line laser for various laser frequency offsets. Laser pulses were emitted horizontally and an accumulation time of laser pulse for each profile is 10 minute. Since signals in the near range were affected by the strong scattering of the outgoing laser pulses from the receiver optics, data were discarded before analysis. The range limit for reliable estimation depends on the atmospheric conditions. The Carrier-to-noise ratio (CNR) of the on-line laser increases with an increase of laser frequency offset. The CNR of the on-line pulses increases with an increase of laser frequency offset. The CNR of the off-line pulses decreased slowly with increasing range up to approximately 20 km. To make vertical XCO<sub>2</sub> measurement, the laser frequency offset of 4.8 GHz was used in consideration of errors on the absorption cross section due to

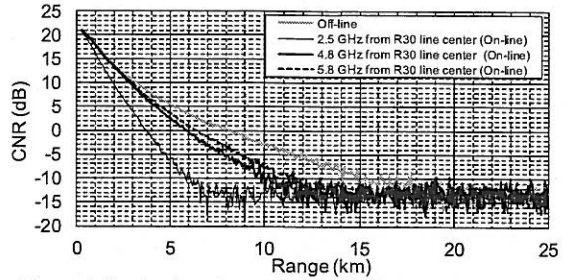


Figure 2 Carrier-to-noise ratio (CNR) of backscattered signal for various laser frequency offsets (2.5, 4.8, 5.8 GHz) and off-line laser.

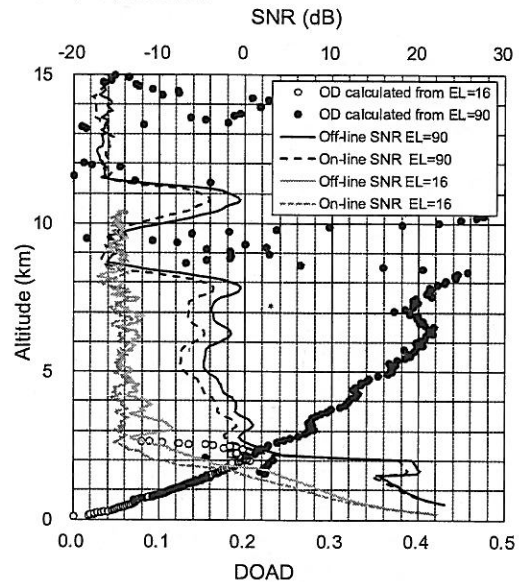


Figure 3 Profiles of differential absorption optical depth (DAOD) and carrier-to-noise ratio observed from 4:08 to 4:33 UT on February 14, 2010

atmospheric pressure and temperature uncertainties.

An example of the vertical profile of the differential optical depth is shown in Figure 3. Airborne in-situ CO<sub>2</sub> measurement was made over NICT to compare with the result of the Co2DiaWiL. The XCO<sub>2</sub> of the in-situ measurement for the integrals between the ground and 1 km was 407.4 ppm. The profiles were obtained by slant and vertical measurements from 4:08 to 4:33 UT on February 14, 2010. The Co2DiaWiL observed aerosol layer and clouds at altitudes of up to 11 km. Clouds are regarded as a hard target and it can help estimate the optical depth. Meteorological data observed by a GPS-sonde launched at the NICT at 3 UT were used to calculate the weighting function. The XCO<sub>2</sub> for the integrals between the ground and 1 km, and 10.5 km were 408.9 ppm and 391.0 ppm, respectively.

## 5. Conclusion

A coherent 2- $\mu\text{m}$  differential absorption and wind lidar with laser offset locking technique was developed to make long-range  $\text{CO}_2$  measurement. The laser frequency offset technique can be set in the range of 2.5 to 6.5 GHz and it enabled to make long-range horizontal and vertical  $\text{CO}_2$  measurements. Experimental slant and vertical measurements were carried out to investigate  $\text{XCO}_2$  in February 2010. The Co2DiaWiL detected aerosol layer and clouds at altitudes of up to about 11 km. The  $\text{XCO}_2$  for the integrals between the ground and 1 km, and 10.5 km were 408.9 ppm and 391.0 ppm.

## 6. References

1. P. J. Rayner and D. M. O'Brien, "The utility of remotely sensed  $\text{CO}_2$  concentration data in surface source inversions," *Geophys. Res. Lett.* 28, pages 175–178, (2001)
2. C. E. Miller, D. Crisp, P. L. DeCola, S. C. Olsen, J. T. Randerson, A. M. Michalak, A. Alkhaled, P. Rayner, D. J. Jacob, P. Suntharalingam, D. B. A. Jones, A. S. Denning, M. E. Nicholls, S. C. Doney, S. Pawson, H. Boesch, B. J. Connor, I. Y. Fung, D. O'Brien, R. J. Salawitch, S. P. Sander, B. Sen, P. Tans, G. C. Toon, P. O. Wennberg, S. C. Wofsy, Y. L. Yung, and R. M. Law, "Precision requirements for space-based  $\text{XCO}_2$  data," *J. Geophys. Res.* 112, page D10314, (2007)
3. F. Chevallier, F.-M. Bréon, and P. J. Rayner, "Contribution of the orbiting carbon observatory to the estimation of  $\text{CO}_2$  sources and sinks: Theoretical study in a variational data assimilation framework," *J. Geophys. Res.* 112, page D09307 (2007)
4. T. Hamazaki, Y. Kaneko, A. Kuze, and K. Kondo, "Fourier transform spectrometer for Greenhouse gases Observing Satellite (GOSAT)," *Proc. of Society of Photo-Optical Instrumentation Engineering*, 5659, pages 73–80 (2005)
5. D. Crisp and co-authors, "The Orbiting Carbon Observatory (OCO) mission," *Adv. Space. Res.*, 34, pages 700-709 (2004)
6. S. Kameyama, M. Imaki, Y. Hirano, S. Ueno, S. Kawakami, D. Sakaizawa, and M. Nakajima, "Development of a 1.6  $\mu\text{m}$  continuous-wave modulation hard-target differential absorption lidar system for  $\text{CO}_2$  sensing," *Opt. Lett.* 34, pages 1513–1515 (2009)
7. J. B. Abshire, H. Riris, G. Allan, C. J. Weaver, J. Mao, Z. Sun, W. E. Hasselbracck, S. R. Kawa, and S. Biraud, "Pulse airborne lidar measurements of atmospheric  $\text{CO}_2$  column absorption," *Tellus*, 62B, pages 770-783 (2010)
8. A. Anediek, A. Fix, M. Wirth, and G. Hert, "Development of an OPO system at 1.57  $\mu\text{m}$  for integrated path DIAL measurement of atmospheric carbon dioxide," *Appl. Phys. B92*, 295–302 (2008)
9. D. Sakaizawa, C. Nagasawa, T. Nagai, M. Abo, Y. Shibata, M. Nakazato, and T. Sakai, "Development of a 1.6  $\mu\text{m}$  differential absorption lidar with a quasi-phase-matching optical parametric oscillator and photon-counting detector for the vertical  $\text{CO}_2$  profile," *Appl. Opt.* 48, pages 748–757 (2009)
10. G. Spiers, "Recent Results and Progress on the Development of a Laser Absorption Spectrometer for Carbon Dioxide Sink and Source Detection," in *Proceedings of the 14th Coherent Laser Radar Conference*.
11. G. J. Koch, J. Y. Beyon, F. Gilbert, B. W. Barnes, S. Ismail, M. Petros, P. J. Petzar, F. J. Yu, E. A. Modlin, K. J. Davis, and U. N. Singh, "Side-line tunable laser transmitter for differential absorption lidar measurements of  $\text{CO}_2$ : Design and application to atmospheric measurements," *Appl. Opt.* 47, pages 944–956 (2008)
12. F. Gilbert, P. H. Flamant, D. Bruneau, and C. Loth, "Two-micrometer heterodyne differential absorption lidar measurements of the atmospheric  $\text{CO}_2$  mixing ratio in the boundary layer," *Appl. Opt.* 45, pages 4448–4458 (2006)
13. S. Ishii, K. Mizutani, H. Fukuoka, T. Ishikawa, B. Philippe, H. Iwai, T. Aoki, T. Itabe, A. Sato, and K. Asai, "Coherent 2- $\mu\text{m}$  Differential Absorption and Wind Lidar with Conductively-Cooled Laser and Two-Axis Scanning Device," *Appl. Opt.* 49, pages 1809–1817 (2010)
14. R. Frehlich, S. M. Hannon, and S. W. Henderson, "Coherent Doppler lidar measurements of winds in the weak signal regime," *Appl. Opt.* 36, pages 3491–3499 (1997)